# Coronal FIP bias: From full-Sun X-ray spectroscopy to imaging spectroscopy

Biswajit Mondal (NASA Postdoctoral Program Fellow at Marshall Space Flight Center, USA)
Santosh V Vadawale, N.P.S. Mithun, Aveek Sarkar, XSM Team (Physical Research Laboratory, India)
Giulio Del Zanna, Helen E Mason (University of Cambridge, UK)
P.S. Athiray (The University of Alabama in Huntsville, NASA Marshall Space Flight Center, USA)
Amy R Winebarger (NASA Marshall Space Flight Center, USA)
Amir Caspi (Southwest Research Institute, USA)

## Summary

The First Ionization Potential (FIP) bias, where elemental abundances of low FIP elements in various coronal structures differ from their photospheric values and may vary over time. X-ray spectroscopic observations of the Sun play a crucial role in studying the spatio-temporal variation and understanding the physical mechanisms behind FIP bias. Recent X-ray spectroscopic observations using the Solar X-ray Monitor (XSM) onboard Chandrayaan-2 in disk-integrated mode have expanded our understanding of FIP bias during solar flares, quiet-Sun X-ray Bright Points (XBPs) and in hot active region (AR) cores. Here we will summarize the findings from these recent studies and briefly discuss the significance of spatially resolved spectroscopic observations in comprehending the FIP bias.

## Chandrayaan-2 Solar X-ray Monitor (XSM)

- Disk-integrated soft X-ray spectrometer of the Sun
- Energy range: 1-15 keV(< M5 class) or 2-15 keV ( > M5).
- Energy resolution: of 175 eV @ 5.9 keV.
- Cadence: 1 second
- Dynamic range: Sub-A to X-9 class flux level
- Good coverage of the Sun during approximately mid-February to mid-May and mid-August to mid-November in a year.
- Operational since September 2019 and continues in perfect health.

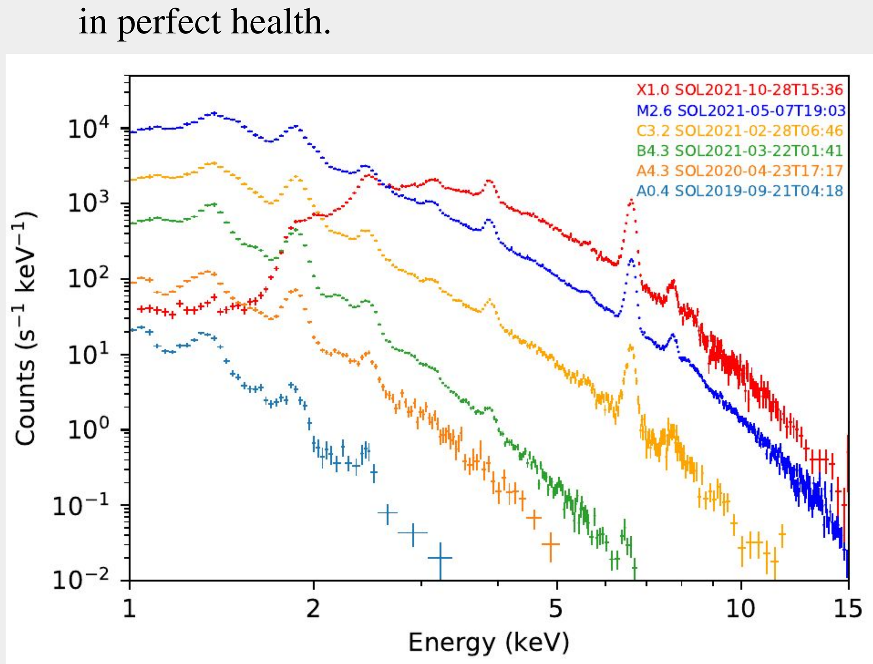


Fig 1. XSM observed spectra for different activity of the Sun. Shanmugam+2020, Mithun+2020

- Spectral fitting the plasma temperature, EM, and elemental abundances with respect to soft X-ray continuum.

XSM website: https://www.prl.res.in/ch2xsm/

## Observations during solar cycle minimum

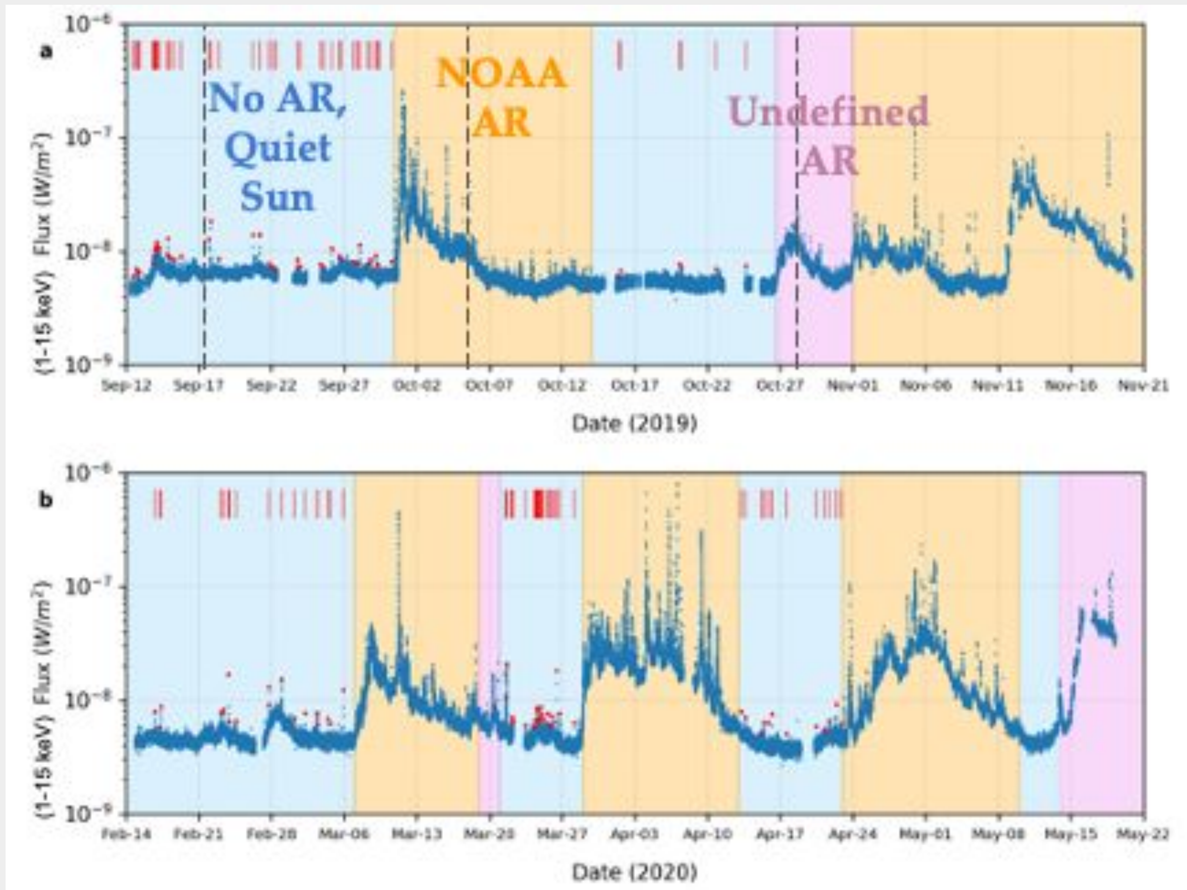


Fig 2. XSM-recorded X-ray flux during the solar cycle 24 minimum. Blue areas indicate periods without active regions (ARs), while orange shading represents single AR presence. Fig 3 displays representative AIA and XRT images for these periods. Red dots denote microflares observed in the quiet Sun outside ARs.

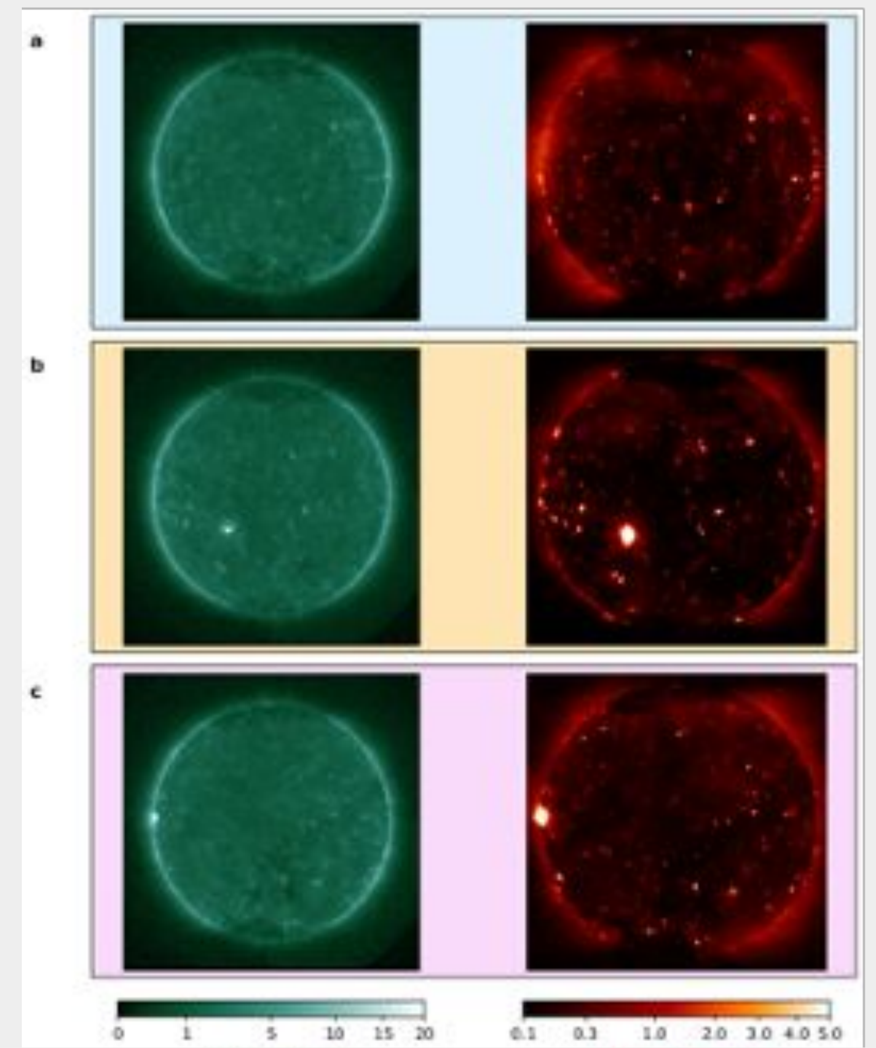

Fig 3. Representative EUV and X-ray images of the different regions marked in Fig 2 as observed by AIA 94A (left) channel and XRT Be-thin filter (right).

- Blue shaded region: No AR provides the opportunity to study quiet solar corona. Most of the X-rays observed by XSM are originated from X-ray Bright Points (XBPs; Vadawale+2021, Mondal+2023b)
- Presence of single AR, where the X-rays are dominated by the AR (orange shaded regions) provides the opportunity to study the evolution of AR.
- Time resolved spectroscopy during the flares provides the evolution of flaring plasma properties

## XBPs and AR

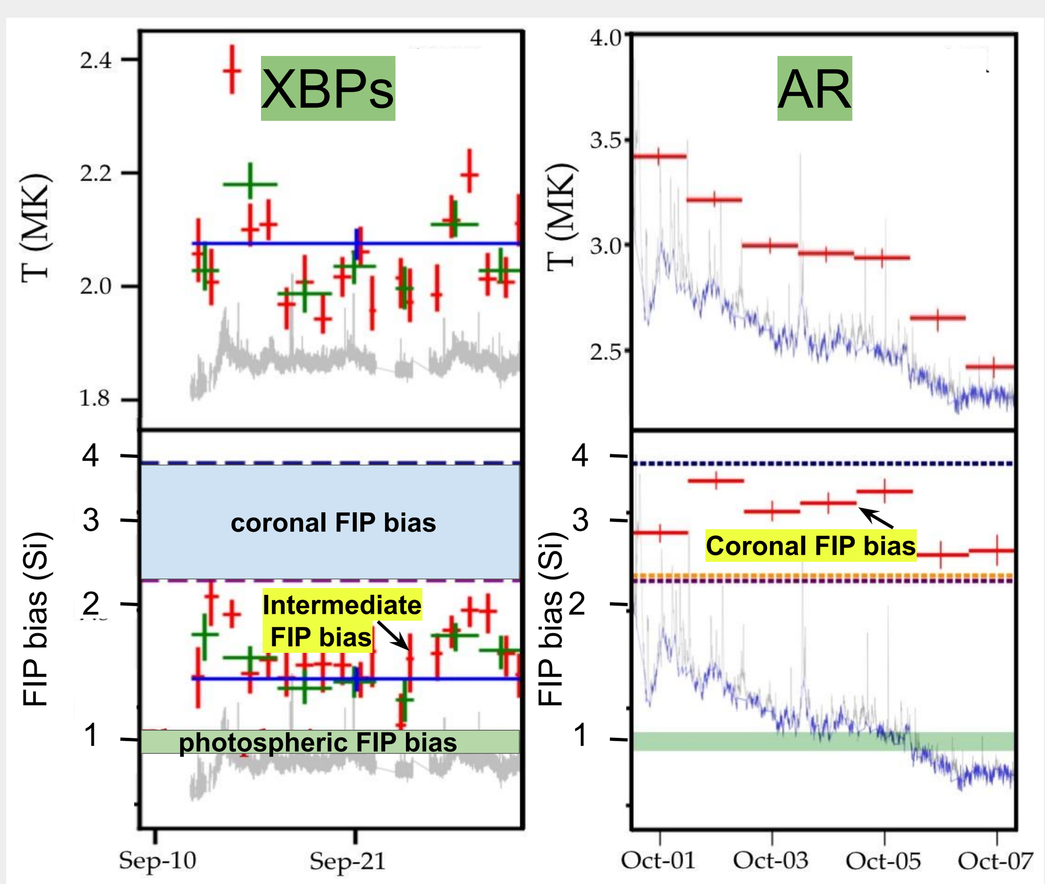


Fig 4. Representative results depicting the evolution of temperature and Si FIP bias for XBPs (left) and AR (right). Note that flaring times are excluded during spectral analysis. The grey curves represent XSM observed flux, while the points with error bars denote the best-fitted parameters. In the left figure, points of varying colors indicate results from fitted spectra integrated over different cadences.

- XBPs FIP bias is in between photospheric and coronal values.
- AR FIP bias is always in the range of coronal values.
- XSM AR abundances agrees with Hinode EIS relative abundance
- Having less magnetic activity of XBPs, their FIP bias is expected to be intermediate according to the Ponderomotive force model of FIP effect.

Vadawale+2021, Zanna+2022, Mondal+2023

## Solar flares

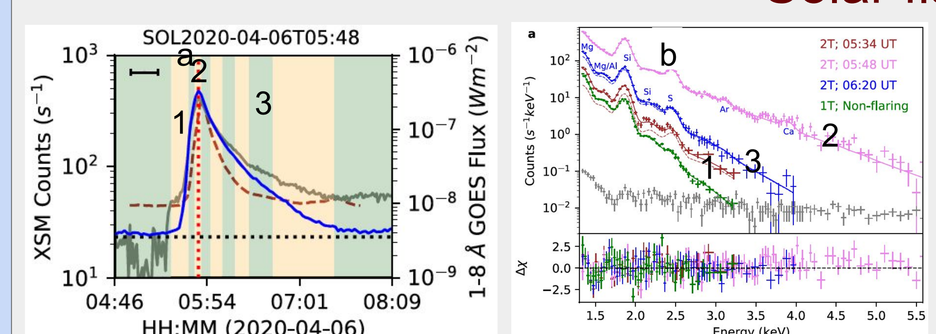


Fig 5. (a) Time selection for time-resolved spectroscopy during a B-class flare. (b) Fitted XSM spectrum during (1) pre-flare, (2) flare-peak and (3) decay phase.

- Impulsive phase shows coronal to near photospheric abundances or FIP bias, indicating chromospheric evaporation.
- Decay phase show a quick (tens of min) transitions from near photospheric to coronal values.
- Quick transition in the decay phase is challenging to explain. Two possible mechanisms are given in Fig 7. It could be due to chromospheric evaporation or/and due the flare-driven Alfven waves.

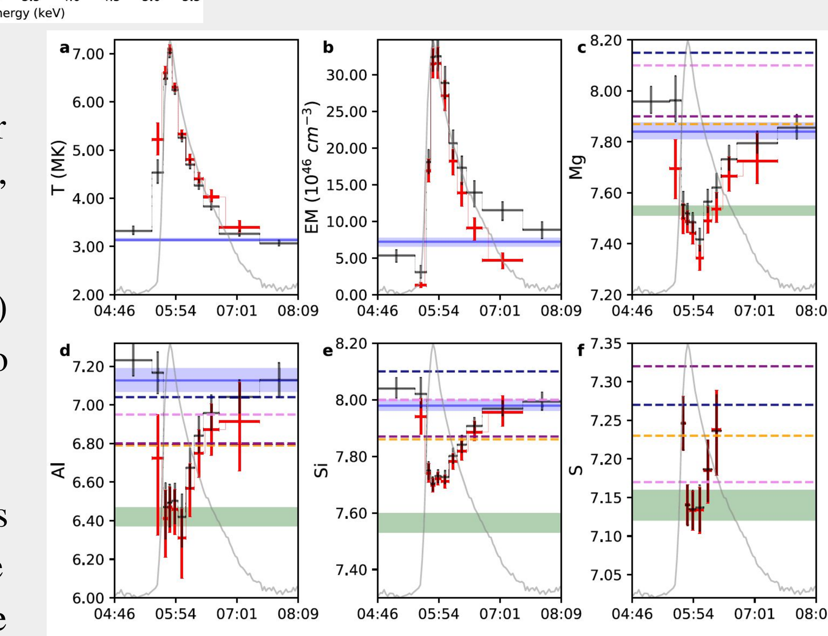


Fig 6. Evolution of plasma temperature (a), EM (b), and abundances (c), Al (d), Si (e), and S (f) during the course of an B-class flare. Flare light-curve is shown in background grey color.

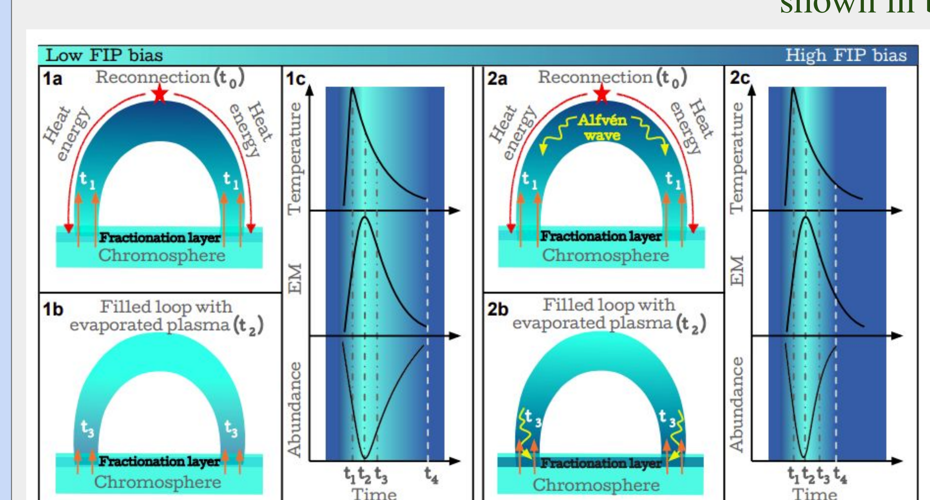


- A similar trends of the abundances are found for much smaller A-class (Nama+2023) flares as well as larger C-class (Mithun+2022) flares .

Fig 7. Cartoon showing two possible mechanisms (1a-1c and 2a-2c) for the observed abundance evolution..

Mondal+2021

## Onset of FIP bias at the emergence of an AR core

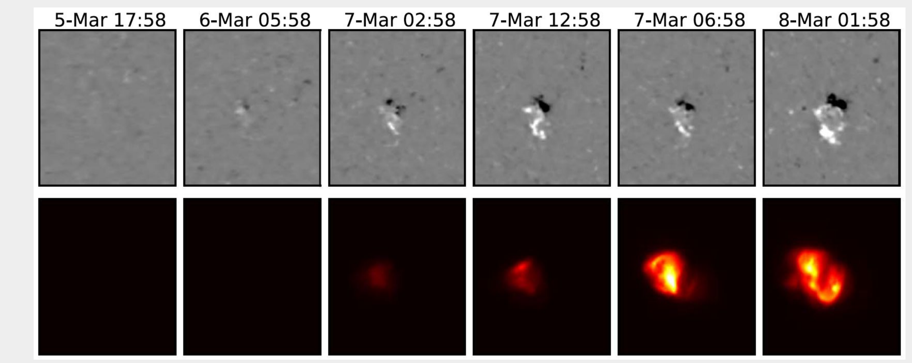


Fig 7. Emergence of AR 12758. Top: SDO/HMI LOS magnetogram. Bottom: Hinode/XRT Be-this images.

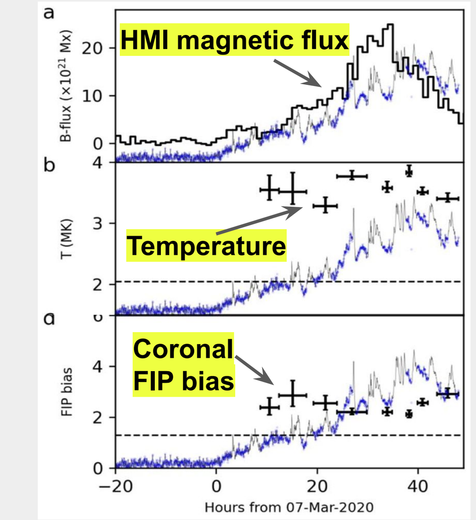


Fig 8. Emergence of AR 12758 as observed by XSM (blue and grey) along with measured parameters (black error-bars) Mondal+2023

- Coronal FIP bias at ~10h of the AR emergence, which is much shorter than the Widing and Feldman (2001) studies.
- It's possible that the time evolution and onset timescale of the FIP effect vary across the AR.

## FIP bias of different elements for XBPs, AR, and Flare peak

- FIP bias is higher for AR compared to XBPs, as expected from the Ponderomotive force model.
- At flare peaks, all elements show a unit FIP bias, indicating chromospheric evaporation.
- Among all low-FIP elements, Al exhibits a higher FIP bias.
- This suggests a possible relationship between the FIP effect and their FIP values.
- Studying Ca, with its FIP between Al and Mg, could provide deeper insights into this phenomenon.

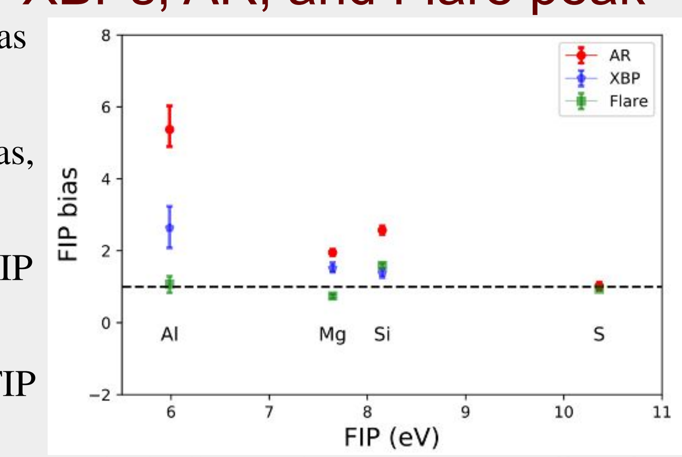


Fig 9. Comparison of the FIP effect for XBPs (blue), AR (red), and flare-peak (green) for different elements.

## Imaging X-ray spectroscopy?

- FIP effect is different for different regions of the Sun, which demands imaging spectroscopic observations.
- Marshall Grazing Incidence X-ray Spectrometer 2 (MaGIXS 2) and Multi-Order X-ray Spectral Imager (MOXSI) onboard CubeSat Imaging X-ray Solar Spectrometer (CubIXSS) will offer high resolution X-ray spectroscopy with moderate imaging information.
- MaGIXS-2, a sounding rocket instrument, offers high energy resolution but limited spatial information for spectral and spatial overlap of ARs in the energy range of ~0.5-2 keV. Valuable for studying the relative abundance of low-FIP versus high-FIP elements
- The MOXSI/CubIXS will provide the spatial and spectral overlap (~0.2-5 keV) of the Sun along with full-disk X-ray images in five filters (similar to XRT/Hinode).
- CubIXSS includes Small Assembly for Solar Spectroscopy (SASS), a disk-integrated X-ray spectroscopic instrument covering the range of ~0.5-100 keV.
- Combining the observations of MOXSI and SASS would provide the spatial variation of FIP effect.
- In the near future, an advanced soft X-ray imaging spectrometer with simultaneous continuum and line measurements will be helpful for spatially varying abundance information relative to hydrogen in an absolute scale.

References:

- Shanmugam, M. et al, Current Science, 118(1):45, 2020
- Mithun, N. P. S. et al., Experimental Astronomy, 51:1, 2021.
- Vadawale, Santosh V. et al., ApJL, 912:L12, 2021
- Del Zanna, G. et al., ApJ, 934:159, 2022.
- Biswajit Mondal; et al., ApJ, 955:146, 2023
- Mondal, Biswajit. et al., ApJ, 920,4, 2021
- N. P. S. Mithun; et al., ApJ, 939:112, 2022.
- Lakshitha Nama; et al., Solar Physics, 298:55 2023.
- Biswajit Mondal; et al., ApJ, 945:37 2023.

Email: biswajit.mondal@nasa.gov